



# Graphene oxide–coated pyrolysed biochar from waste sawdust and its application for treatment of cadmium-containing solution: batch, fixed-bed column, regeneration, and mathematical modelling

Vijoyeta Chakraborty<sup>1</sup> · Papita Das<sup>2,3</sup> · Pankaj Kumar Roy<sup>1</sup>

Received: 30 August 2020 / Revised: 4 November 2020 / Accepted: 13 November 2020 / Published online: 8 January 2021  
© Springer-Verlag GmbH Germany, part of Springer Nature 2021

## Abstract

Cadmium being a heavy metal, which is also a known pollutant, had a wide variety of usage in many industries like electroplating industries, phosphate fertilizers, batteries, mining, stabilizers, pigments, and alloys. In this study, sawdust was used to produce the nanocoated adsorbent. Sawdust is non-hazardous low-cost waste materials and easily available. Thermally activated biochar was produced from sawdust and coated with graphene oxide nanomaterials in two different methods, and the synthesized nanocomposite was used to remove cadmium present in solution. Batch study was performed to optimize different parameters for better removal. Experiments were performed and the best condition optimized for removal of cadmium was found to be pH 7.5 and temperature 35 °C or 308.15 K, with 1 g/L adsorbent dose, and within 2 h, i.e. 120 min, above 55.68 mg/g removal capacity was attained with initial metal concentration of 50 mg/L. The modified saw dust composite was more effective in removal of cadmium than the normal sawdust-based composites. The characterization of the nanocomposite was done to know the internal structure of the composite. The continuous fixed-bed column study was performed, and the study followed Admas–Bohart model. The batch and column study results showed that this nanocoated composite can be an alternative for the treatment of pollutant present in the solution. The regeneration of the composite showed a sustainable use of the composite for the treatment of pollutant.

**Keywords** Cadmium · Adsorption · Pyrolysed · Batch study · Fixed bed · Column study · Regeneration

## 1 Introduction

Wastewaters contaminated with metal ions are major environmental issues. The bio-accumulative property and non-biodegradability of metal ions are toxic and hazardous for the living system (Garg et al., 2016). International Agency for Research on Cancer (IARC, 1974) had categorized cadmium as highly toxic and carcinogenic in nature. The exposure of Cd (II) will cause severe detrimental effect to many body

parts, like kidney, pancreas, prostate, lung, bones, and liver. The disease caused by cadmium exposure is known as itai-itai [1]. Other than this disease, some chronic and acute diseases like pulmonary problems, skeletal deformity, renal damage, nausea, behaviour disturbance, kidney stone formation, cognitive impairment, and protein metabolism disruption may be caused by exposure to cadmium [2, 3]. The discharge of Cd (II) from various industrial processes was studied earlier; industries which discharge cadmium are mining, pigments, phosphate fertilizers, smelting, alloy industries, electroplating, and sewage sludge and nickel and cadmium batteries [4]. Their effluent water contains a high amount of Cd (II).

In recent times, there is a stringent norm regarding pollution control system, which is demanding application of innovative technologies in wastewater treatment [5]. Many technologies including membrane filtration, ion exchange, reverse osmosis, reduction, photo-catalysis, flocculation, adsorption, and precipitation advance oxidation were used previously in many research works for removal of metal ion from solution.

✉ Papita Das  
papita.das@jadavpuruniversity.in

<sup>1</sup> School of Water Resources Engineering, Jadavpur University, Kolkata, India

<sup>2</sup> Department of Chemical Engineering, Jadavpur University, Kolkata, India

<sup>3</sup> School of Advanced Studies in Industrial Pollution Control Engineering, Jadavpur University, Kolkata, India

Within all these technologies, the fastest simplest, globally accepted, economical, and eco-friendly technique is adsorption. But the success of the adsorption technique is largely depending on the process parameters used for removal of metal ion and the property of the adsorbent which will be used for treatment of contaminated waste water.

The uses of bio-nanocomposite in application of wastewater treatment are gaining constant attention from the researchers. The bio-nanocomposites were mainly made up of two or more materials on base material, which would preferably be any biomaterials like sawdust, sugarcane bagasse, rice husk, orange peel, and many other lignocellulosic biomaterials ([6–9, 10]); the removal of Cd (II) was also done with fly ash, spent grain etc. [11]. The surfaces of these biomaterials may be coated with nanomaterial like graphene oxide and magnetic nanoparticles [12, 13].

This paper is based on removal of cadmium using treated sawdust coated with nanoparticle. The sawdust being a lignocellulosic waste contains many oxygen-containing functional groups, which provided good surface characteristics [14], and the filler material used was graphene oxide which was known for its highly porous structure and surface active functional groups. The composites prepared from these components contain higher surface characteristic. A comparative study was performed by using biochar obtained by pyrolysing sawdust, modifying the composite with chemical treatment, and coating with GO in hydrothermal reactor [15]. In this study, the highest removal capacity of cadmium among the adsorbents was optimized and further study was performed. Feasibility of the composite in industrial application was estimated using column study. The functional group analysis was performed, and the functional group responsible for removal using FTIR and other surface characteristics was optimized using SEM, TGA, BET, and XRD analysis.

## 2 Materials and methodology

### 2.1 Materials

Cadmium nitrate ( $\text{Cd}(\text{NO}_3)_2 \cdot 4\text{H}_2\text{O}$ ) (Merck), graphene oxide (GO) (Platonic India Private Ltd), sawdust, sodium hydroxide (NaOH) (Merck), hydrochloric acid (HCl) (Merck), ethanol (Merck), acetone (Merck), hydrazine hydrate (Merck), distilled water, Whatman no. 1 filter paper. All chemicals used were lab grade.

### 2.2 Cadmium stock preparation

1.37 gram of cadmium nitrate powder was dissolved in 1 L distilled water to make 500 mg/L cadmium stock solution. The experiments were conducted by diluting this stock solution.

### 2.3 Preparation of surface-functionalized GO-coated biochar nanocomposite

The raw sawdust was washed with distilled water and treated with 0.01 N NaOH for 2 h. Then, the treated sawdust was washed repeatedly using distilled water until the pH was maintained at 7. Then, the chemically treated sawdust was dried in a vacuum drier for 12 h. Five grams of treated sawdust was taken in a conical flask and dispersed in 200 mL acetone, then sonicated for 2 h. Simultaneously 50 mg of GO was sonicated in 50 mL acetone solution. Then, both of the solutions containing sawdust and GO were mixed together and stirred in a magnetic stirrer for 1 h and kept into a Teflon-coated autoclaved reactor and 1 mL hydrazine hydrate was added to it, and then refluxed for 18 h at 140 °C. The resultant mixture was then filtered and washed repeatedly with ethanol until the pH was maintained at 7. Then, the composite was vacuum dried to obtain fine powder. The composite was pyrolysed at 700 °C for 2 h. The composite prepared was then stored into an air tight container (mSDGO). The activated carbon obtained by pyrolysing the GO-modified sawdust at 700 °C was initially screened to optimize the activation temperatures. The carbonization temperature was selected by screening different temperatures from 300 to 900 °C. When the biomass was treated at highest temperature, i.e. 900 °C, some loss of biomass and ash formation was observed, which was not acceptable in preparation of activated carbon. So the temperature of carbonization was maintained at 700 °C. This temperature optimization study was done in our previous work [7]. The second composite was prepared using thermally modified sawdust with surface functionalized with graphene oxide (SDGO); the process was described here briefly. The raw sawdust was washed with distilled water to remove any dust or dirt present in its surface, and then treated with 0.01 N NaOH for 4 h. After the alkali, the modified sawdust was washed until the pH of the solution became neutral. Then, the treated sawdust was pyrolysed at 700 °C for 1 h. The composite was prepared by mixing 300 mg graphene oxide (GO) in 50 mL acetone solution, which was sonicated for 1 h. On the other hand, 10 g biochar was stirred in 150 mL acetone solution separately for 1 h. Then, both the solutions were mixed and sonicated for 2 h. The resultant composite (SDGO) was dried in a vacuum drier for 24 h and stored in an air tight container. The resultant nanocomposites obtained from these preparation procedures were effective in removing cadmium from the experimental solution. The composite prepared by using plant-based biomass provides the active functional groups from its natural composition. The coating of these biomass with GO enhanced the surface functional groups on the adsorbent.

## 2.4 Batch adsorption study

Five different parameters were optimized in this study, namely pH, temperature, adsorbent dosage, contact time, and metal ion concentration. The whole experiment of the batch study was conducted using 50 mL of the metal ion solution. The pH of the solutions were maintained by using 0.01 N NaOH and 0.01 N HCl. Variation of dose, pH, and temperature was studied to optimize the parameters. For study of contact time, the samples were collected at specific time interval. Lastly, the initial metal ion concentration was studied with different concentrations of cadmium nitrate solution. The concentration taken for this study was 50 mg/L, 100 mg/L, 250 mg/L, and 500 mg/L. It should be noted here that when one parameter was optimized, the other parameters were kept constant. The conical containing test solutions were kept in an incubator shaker for minimum of 2 h (120 min) and maximum 24 h (1440 min) at 150 rpm. After studying each parameter, the solution was filtered using Whatman no. 1 filter paper and the removal efficiency of the adsorbents was estimated by using inductively coupled plasma–optical emission spectroscopy (ICP-OES) (Perkin Elmer, USA). A comparative study was done with both of the synthesized nanocomposites. For estimation of cadmium into the solution, a standard curve of the metal ion solution was stored in ICP-OES for future reference.

The isotherm experiments were carried out for different cadmium concentrations for a period of 120 min. The studies of adsorption kinetics were done with 50 mg/L of initial cadmium solution, and the samples were taken at time interval of 15 to 120 min. For the study of thermodynamics, different temperatures were studied (298.15 to 313.15 K). The capacities of the adsorbent in removing the metal from the experimental solution were calculated using the following equation:

$$q_e = (C_0 - C_e) \times \frac{v}{m} \quad (1)$$

The adsorption capacity of the adsorbent was denoted by  $q_e$  (mg/g),  $C_0$  was the initial Cd (II) concentration, and  $C_e$  was the equilibrium concentration of Cd (II). The volume of the solution was denoted by  $v$  (mL), and the mass of the adsorbent used was denoted by  $m$  (mg).

## 2.5 Fixed packed bed column study

For the study of continuous fixed-bed column, columns were taken of 3 cm diameter and 50 cm in length. A flow rate of 2.5 mL of inlet and outlet flow was maintained throughout the experiment. With the help of the peristaltic pump (Reviara, India), the metal ion solution was poured into the column. The results of this study were collected in triplicate, and the concentration of Cd (II) ion concentration in mg/L was measured in ICP-OES. This study was performed at different metal

concentrations (50 mg/L, 100 mg/L, and 250 mg/L) and three different bed heights (1 cm, 2 cm, and 3 cm). The whole experiment was conducted in room temperature. The columns were studied until it reaches the saturation point.

Admas–Bohart model and Thomas model were applied to know the dynamic behaviour of the column. The break-through curve was a very important parameter for the column analysis which could be obtained by analysing these models [16]. The breaks through curves were obtained from the graph plotted against  $C_t/C_0$  vs time. Here  $C_t$  was the concentration of metal ion (mg/L) at liquid phase at time ( $t$ ), whereas  $C_0$  means the concentration of initial metal ion solution (mg/L). The following equations were used to denote these models.

Admas–Bohart model [17]:

$$\ln\left(\frac{C_t}{C_0}\right) = k_{AB}C_0t - k_{AB}N_0\left(\frac{Z}{v}\right) \quad (2)$$

Thomas model [18]:

$$\ln\left[\left(\frac{C_0}{C_t}\right) - 1\right] = \left(\frac{k_{TH}q_0m}{F}\right) - \left(\frac{k_{TH}C_0V_{eff}}{F}\right) \quad (3)$$

$k_{AB}$  denotes kinetic constant for Admas–Bohart model ( $L \text{ mg}^{-1} \text{ min}^{-1}$ );  $N_0$  denotes maximum volumetric sorption capacity ( $\text{mg L}^{-1}$ ). The flow rate of the metal ion was denoted by  $v$  ( $\text{cm min}^{-1}$ ) and the  $Z$  denotes the bed height of the column (cm).  $k_{TH}$  was denoted as Thomas rate constant ( $\text{mL mg}^{-1} \text{ min}^{-1}$ ). The equilibrium of mg of Cd (II) ion uptake was denoted by  $q_0$  ( $\text{mg g}^{-1}$ ). The total mass of nanocomposite used was denoted by  $m$  (g).  $F$  denotes the volumetric rate of metal ion flow ( $\text{mL min}^{-1}$ ), and  $V_{eff}$  denoted the volume of effluent discharged (mL).

The column study was used as a replica for industrial usage. This was very helpful in designing a pilot scale plant.

## 2.6 Characterization of the adsorbent

The functional groups present within the adsorbent were characterized using Fourier transformation infrared spectroscopy (FTIR) (PerkinElmer Spectrum Version 10.4.4, Waltham, USA); the structural morphology of the adsorbent was studied using scanning electron microscope (SEM) analysis (ZEISS EVO-MA 10, Carl Zeiss Microscopy, USA); X-ray diffraction (XRD) analysis (PANalytical X-PERT PRO, Malvern Panalytical) was done to know its crystallinity; the thermal stability or heat sensitivity was done by thermo-gravimetric analysis (TGA) (STA 6000, PerkinElmer, USA); lastly, the surface area was analysed by  $N_2$  adsorption method using BET (Brunauer–Emmett–Teller) analysis (Autosorb-iQ-MP/XR, Quantachrome Instruments, USA).

## 2.7 Reutilization study

The composites once used in batch study were reused again for Cd (II) ion removal for five consecutive cycles, and adsorption capacity for the reused material was calculated and reutilization of the composite was noted. The composite was treated with slightly basic solution 0.1 N NaOH, and used for the next time.

## 3 Results and discussions

### 3.1 Batch adsorption experiment

#### 3.1.1 Effect of pH on Cd (II) adsorption

The adsorbents had shown an effective removal of cadmium from aqueous solution. The pH studied were ranges from pH 2 to pH 10; with increased in pH of the solution, the removal of Cd (II) had also increased. But it was observed that after pH 8 the removal of the metal ion became same. So for further experiment, the pH of the solution was made between pH 6 and pH 8. pH 8 was showing maximum adsorption capacity. The adsorption capacity of cadmium had increased from 12.8 mg/g to above 54.73 mg/g from pH 2 to pH 8; above pH 8, the removal of Cd (II) became stagnant. Similar trend was observed with the other modified composite (mSDGO). At pH 2 the adsorption capacity was 5.1 mg/g which increased till 44.52 mg/g. The surfaces of the adsorbents used in this study were highly protonated at lower pH, so no active sites for adsorption of Cd (II) ion were present. As the pH became neutral, the protonation of the active sites was lowered so more active sites for adsorption are exposed and higher removal of cadmium was observed. At higher pH, removal became high. At higher pH, the cadmium ions forms its oxide form and got precipitated. So the pH of the study was maintained as neutral to slightly acidic pH the negative charged functional group were present at the adsorbent surface which could bind with the metal ion, the pH 6 was maintained throughout the experiment [13, 19]. The removal of Cd (II) is shown in Fig. 1.

Different forms of cadmium species (Cd (II)) were mainly found in different pH in aqueous solution, namely  $\text{Cd}^{+2}$ ,  $\text{Cd}(\text{OH})^+$ ,  $\text{Cd}(\text{OH})_2$ ,  $\text{Cd}(\text{OH})_3^-$ , and  $\text{Cd}(\text{OH})_4^{-2}$  [4, 13]. The lower pH provides a protonated surface on the adsorbent. So there exists an electrostatic repulsive force between adsorbent surface and Cd (II) ion. As the pH increased in the solution, the degree of protonation decreases and it was found to be neutral or zero at  $\text{pH}_{\text{pzc}}$ . The SDGO had lower  $\text{pH}_{\text{pzc}}$  than the modified SDGO (mSDGO) (Fig. 2). The mSDGO had its point zero charge at pH 7.5; the  $\text{pH}_{\text{pzc}}$  of the SDGO was done in our previous work [20]. The  $\text{pH}_{\text{pzc}}$  of this mSDGO was in neutral range of pH, so at higher pH, the Cd (II) ion

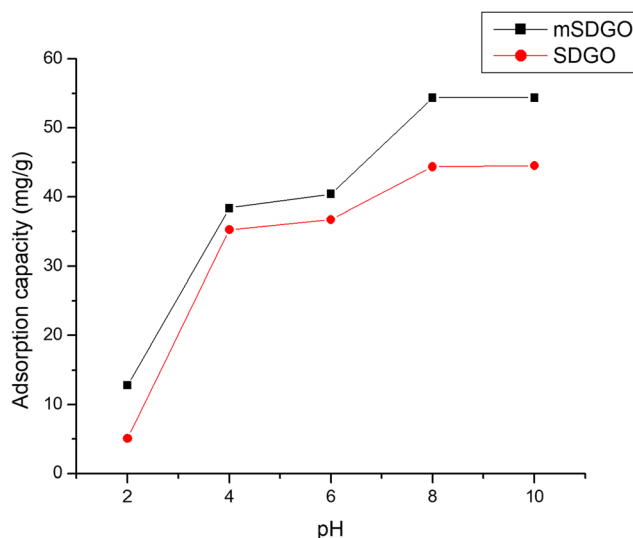


Fig. 1 Effect of pH on removal of Cd (II) ion by SDGO and mSDGO

precipitates as  $\text{Cd}(\text{OH})_2$  increased its removal capacity at the range in basic pH. So for the further study pH 7.5 was maintained thoroughly.

#### 3.1.2 Effect of temperature

The effect of temperature in Cd (II) removal was studied (298.15 to 318.15 K). Both the composites, i.e. SDGO and mSDGO, showed an increase in adsorption capacity with increase in temperature. The adsorption capacity increased from 31.16 mg/g to 56.28 mg/g for mSDGO and from 26.48 mg/g to 44.56 mg/g for SDGO. The increase in the performance of adsorbents with increase in temperature could be due to higher amount of Cd (II) diffusion on to the external surface and pores of the adsorbent. The increased temperature helps in lowering the thickness of the boundary of the adsorbent,

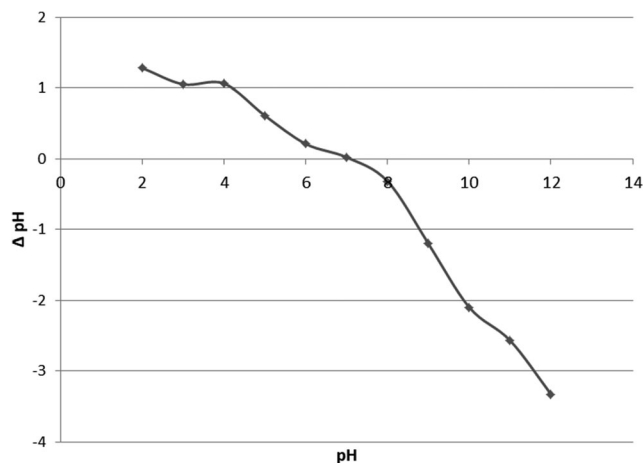
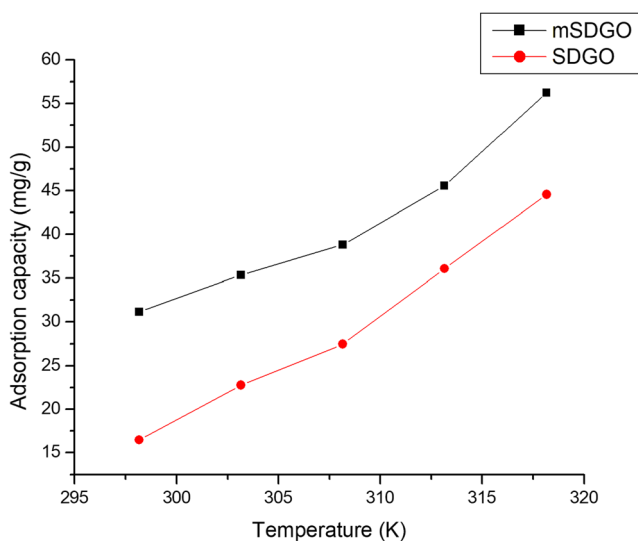


Fig. 2  $\text{pH}_{\text{pzc}}$  of mSDGO

which in turn reduces the metal transfer resistance property [21, 22]. The composites were not affected with increasing temperature, so it could be inferred from this result that the composites have good thermal stability. The increase in temperature increases removal capacity of the adsorbents. This can be due to the fact that with increase in temperature there was diffusion of cadmium ion to the external surface [13]. The surface functional group could become less active in low temperature. With increase in temperature, the pore space also opens up and the metal ion got adsorbed, which was showing higher removal percentage (Fig. 3).

### 3.1.3 Effect of amount of adsorbent used for removal of Cd (II)

The optimum adsorbent dosage was studied using different doses of adsorbent. The adsorbent dose was optimized using dosage from 1 g/L to 10 g/L; the increase in adsorbent dosage gave increased amount of active surface function groups on the adsorbent surface for metal binding site. Both composites had high amount of active surface functional group, since the sawdust was coated with graphene oxide, which contains abundant oxygen-containing surface functional groups like hydroxyl and carboxyl, the SDGO had abundant of these surface active functional groups. The mSDGO had more of these groups since it was also modified with hydrazine hydrate; higher numbers of surface active functional groups were present in this adsorbent. The whole experiment was done at pH 7.5, and at temperature 308.15 K. The adsorbent capacity decreased with increase in adsorbent dose; with higher amount of adsorbent dosage, there may be agglomeration of adsorbent in its surface; due to this congestion, the binding sites of these adsorbents were preoccupied with other adsorbent molecules, so the metal could not bind properly with the adsorbent surface [23, 24]. This mechanism reduces the metal



**Fig. 3** Effect of temperature on Cd (II) ion removal by SDGO and mSDGO

uptake capacity of the adsorbent affecting its adsorption capacity. The adsorption capacity decreased from 53.45 mg/g to 6.26 mg/g for mSDGO and 44.75 mg/g to 3.68 mg/g for SDGO. The adsorption capacity decreased but the per cent removal increased from 84.33% to 98.86% for mSDGO and 70.60% to 89.64% for SDGO (Fig. 4). The adsorbent capacity was high for 1 g/L of adsorbent dose. So for further experiment this dosage was kept constant.

### 3.1.4 Effect of cadmium concentration on adsorbent

Different concentrations of Cd (II) ion solution were studied in this experiment. The whole experiment was performed with 50 mg/L of metal ion solution. In this experiment, concentrations up to 500 mg/L were studied. The studied concentrations were 50 mg/L, 100 mg/L, 250 mg/L, and 500 mg/L. The increase in concentration resulted in increase in adsorption capacity of the adsorbents. The availability of metal ion for the specific amount of adsorbent provided more chance for metal ion to get adsorbed into the pores of the adsorbents and binding with the active sorption sites. The high amount of mass transfer process had provided higher adsorption capacity of the adsorbent. The whole experiment was done using 1 g/L of adsorbent dose. The pH was maintained at 7.5; the experiment was performed in 308.15 K. The adsorbent capacity was increased from 51.74 mg/g to 145.7 mg/g for mSDGO and from 44.82 mg/g to 88.2 mg/g for SDGO, shown in Fig. 5. The adsorption capacity was more for mSDGO than SDGO; this could be due to increased diffusion of metal ion across the boundary that was formed by accumulation of metals along the surface of the adsorbent. The competitive adsorption with in the metal ion was influenced by the surface area of the adsorbent. The BET analysis showed that the surface of mSDGO was much higher than SDGO. The result from this

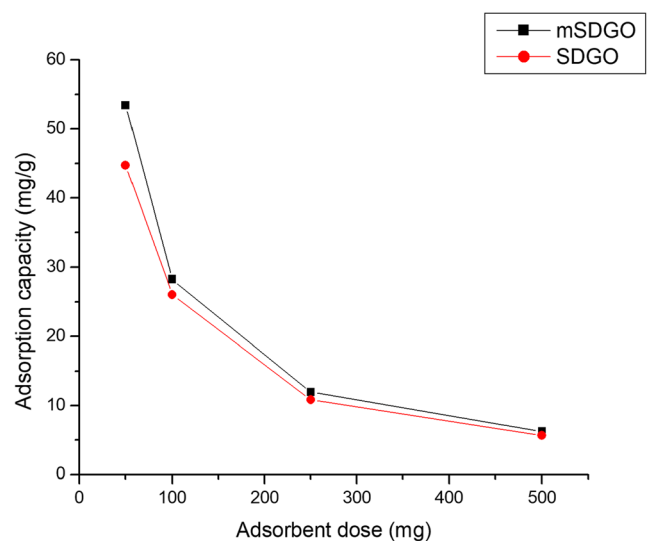


**Fig. 4** Effect of adsorbent dose on Cd (II) ion removal by SDGO and mSDGO



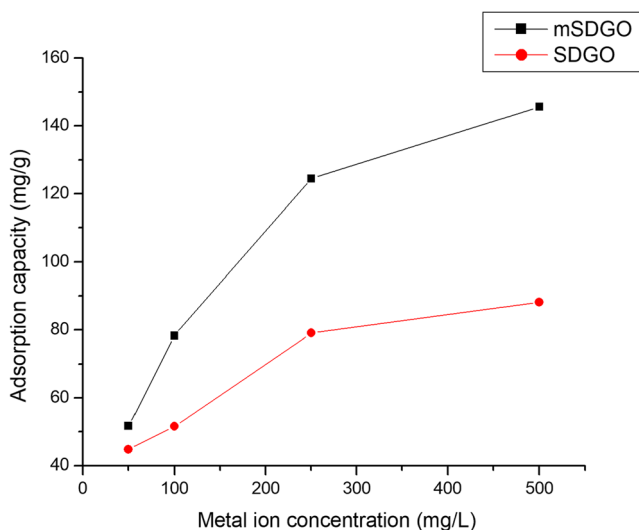


**Fig. 5** Influence of different concentration Cd (II) ion removal on SDGO and mSDGO

analysis also suggests that the efficiency of mSDGO was more than SDGO. The possible reason could be the higher surface to volume ratio of the adsorbent [25]

### 3.1.5 Effect of contact time

This study was done to know the equilibrium obtained from this study. The study was performed at 308.15 K temperature, with pH 7.5; adsorbent used in this study was 1 g/L. 50 mg/L Cd (II) solution was used here. The study was done with both the adsorbents, and a similar trend was observed that a high adsorption capacity was attained within 60 min of this experiment (Fig. 6). After this time the adsorption capacity had slightly increased. The final equilibrium was attained within 120 min of the experiment. The results obtained from these

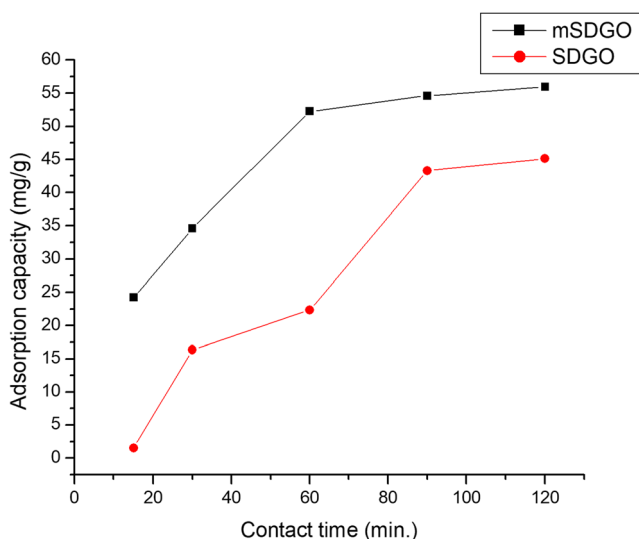


**Fig. 6** Effect of contact time on Cd (II) ion removal by SDGO and mSDGO

experiments suggest that the active surface functional groups were initially free for Cd (II) adsorption, but with increase in time, they got occupied with the metal ions within 120 min of the experiment. So the equilibrium was reached within this time; no further surface interaction or adsorption would take place after this time (Zhao et al., 2015).

### 3.1.6 Isotherm study

In this study the interaction between the adsorbate and the nanocomposite was studied. The surface binding of the nanocomposite with the metal ion and the mechanism behind it could be established using these isotherm studies. Here mainly two isotherms were studied, Langmuir isotherm and Freundlich isotherm. The models were represented using the following linear equation.

Langmuir isotherm model:

$$\frac{C_e}{q_e} = \frac{1}{q_{\max}b} + \frac{C_e}{q_{\max}} \quad (4)$$

Freundlich isotherm model:

$$\log q_e = \log k_f + \frac{1}{n} \log C_e \quad (5)$$

The  $q_{\max}$  (mg/g) was the highest adsorption limit for Cd (II) ion removal.  $b$  (mg/L) denotes Langmuir constant,  $K_f$  (mg/g(L/mg)<sup>1/n</sup>) denotes Freundlich constant. The favourability of adsorption was suggested if the value of ‘ $n$ ’ was in between 1 and 10 (Kataria et al., 2016). ‘ $n$ ’ was denoted as heterogeneity factor. The parameters for these isotherm models were calculated from graphs obtained by plotting  $\frac{C_e}{q_e}$  vs  $C_e$  for Langmuir model and  $\log q_e$  vs  $\log C_e$  for Freundlich model. Results obtained from this analysis are given in Table 1.

The mSDGO had higher adsorption capacity than SDGO, so the further model analysis was done for that nanocomposite only. With high value of correlation coefficient ( $R^2$ ), Freundlich model fits the experimentation on good agreement. The  $R^2$  value was found to be 0.9937 which was more than

**Table 1** Parameters obtained from Langmuir and Freundlich isotherm modelling

Model	Parameters	Value obtained
Langmuir	$q_0$ (mg/g)	153.846
	$K_L$ (L/mg)	0.0290
	$R_L$	0.6386
	$R^2$	0.988
	Freundlich	$K_F$
	$N$	3.856
	$R^2$	0.994

Langmuir isotherm model ( $R^2 = 0.9883$ ). The  $n$  value obtained from this model was 3.856, which was more than 1, and it could be suggested from this value that the adsorption was favourable in this experiment. The process of adsorption could be chemical reaction between the metal ion and the active surface functional group. The chemisorption was the main driving force behind the adsorption mechanism suggesting multilayer adsorption process.

### 3.1.7 Kinetics study

The rate at which the process of Cd (II) adsorption took place was estimated using kinetic study. Pseudo-first-order and pseudo-second-order kinetics were studied to know the mechanism of adsorption. This study was done by taking experimental readings for 120 min, at the time interval of 15 min. The following linear equations were obtained to know kinetics of adsorption.

Pseudo-first-order kinetics:

$$\log(q_e - q_t) = \log q_e - \left(\frac{k_1}{2.303}\right)t \tag{6}$$

Pseudo-second-order kinetics:

$$\frac{t}{q_t} = \frac{1}{k_2 q_e^2} + \frac{t}{q_e} \tag{7}$$

The equilibrium concentration ( $q_e$  (mg/g)) and at time of contact ( $q_t$  (mg/g)) was calculated in this experiment. The rate constant from pseudo-first-order  $k_1$  ( $\text{min}^{-1}$ ) was obtained from plotting the linear graph of  $\log(q_e - q_t)$  vs  $t$ . The  $R^2$  was also calculated using this graph; the  $q_e$  was also calculated. The second-order kinetics was also studied by plotting the graph between  $t/q_t$  vs  $t$ . The rate constant  $k_2$  ( $\text{g mg}^{-1} \text{min}^{-1}$ ),  $q_e$ , and  $R^2$  were calculated using this linear equation of the second-order kinetics. The results obtained from kinetics study are shown in Table 2. The pseudo-first-order kinetics had high  $R^2$  value (0.988) than pseudo-second-order which had  $R^2$  value (0.9678) lower than the first order. But the  $q_e$  value of the second-order kinetics was near to the value obtained from the experimental  $q_e$  value; in case of first-order kinetics, the experimental  $q_e$  value was not closer to the calculated  $q_e$  value. So for this experiment, the pseudo-second-order

kinetics was well fitted, suggesting the total adsorption process was chemisorption in nature (Table 2). Strong chemical bonding between the Cd (II) ions was chemically bonded with the active surface functional group.

### 3.1.8 Thermodynamics study

This study was done with five different temperatures from 298.15 to 313.15 K. As the temperature increased, the adsorption capacity increased from 31.16 mg/g to 56.28 mg/g. The adsorption process was mainly of two types, endothermic and exothermic, and it could be of spontaneous and non-spontaneous nature. The values of Gibb's free energy ( $\Delta G^\circ$ ), enthalpy ( $\Delta H^\circ$ ), and entropy ( $\Delta S^\circ$ ) was also calculated using this study. The calculations were done using these following equations:

$$\Delta G^\circ = -RT \ln K_d \tag{8}$$

$$\Delta G^\circ = \Delta H^\circ - T \Delta S^\circ \tag{9}$$

$$K_d = \frac{C_a}{C_e} \tag{10}$$

$$\ln K_d = \frac{\Delta H^\circ}{RT} + \frac{\Delta S^\circ}{R} \tag{11}$$

$R$  denotes universal gas constant ( $8.314 \text{ J mol}^{-1} \text{ K}^{-1}$ ), equilibrium constant was denoted by  $K_d$ , and  $T$  denotes the temperature in kelvin (K). The Cd (II) ion concentration adsorbed on the surface of the adsorbent (mg/L) was denoted by  $C_a$  and equilibrium concentration of Cd (II) was denoted by  $C_e$  (mg/L). The graph plotted for  $\ln K_d$  vs  $1/T$  was used for the calculation of all the thermodynamics parameters. The spontaneous adsorption process was indicated by the negative value of  $\Delta G^\circ$ . The  $\Delta H^\circ$  value obtained from the plotted graph was positive indicating the whole process to be endothermic in nature. It can be said that the Cd (II) ion adsorption on the surface of the nanocomposite (mSDGO) would increase as temperature increases [1]. By analysing the results, the degree of randomness increased as the surface interaction between adsorbent and adsorbate, i.e. mSDGO and Cd (II) ion, increased. This could be stated from the positive  $\Delta S^\circ$  value obtained from the plotted graph. The increase in randomness increased the affinity of the Cd (II) ion toward mSDGO [22].

**Table 2** Parameters obtained from kinetics study

Rate kinetics model	Parameters for kinetics modelling			
	Rate constant	$q_{\text{exp}}$	$q_{\text{ecal}}$	$R^2$
Pseudo-first-order	$k_1 = 0.0414$	55.96	5.7488	0.9883
Pseudo-second-order	$k_2 = 0.00637$	55.96	68.966	0.9678

**Table 3** Parameters obtained from thermodynamics study

Temperature (K)	$\Delta G^\circ$ (kJ/mol)	$\Delta H^\circ$ (kJ/mol)	$\Delta S^\circ$ (kJ/mol)
298	-17.071	78.977	0.323
303	-18.030		
308	-18.919		
313	-20.497		
318	-23.937		

The result of this study is shown in Table 3. The results obtained could suggest that the process was spontaneous and favourable for adsorption.

### 3.1.9 Characterization of the adsorbent

The batch adsorption study suggests that the mSDGO was more capable for adsorption of Cd (II) ion than SDGO, so the further characterization of mSDGO was done to know the internal structure and morphology and surface characteristics of the adsorbent, which was responsible for better efficiency of mSDGO.

**FTIR analysis** The presence of active surface functional group in the adsorbent surface was estimated by using FTIR analysis (Fig. 7a). Five distinct peaks were obtained by FTIR analysis; the peak at  $1081\text{ cm}^{-1}$  indicated presence of C-O group of –

OCH<sub>3</sub> group usually found in biomass containing lignin [25, 26];  $1421\text{ cm}^{-1}$  indicated C=O stretching of carboxylate group [26]. The peak obtained at  $3255\text{ cm}^{-1}$  suggested a strong presence of –OH group and also the presence of –NH<sub>2</sub> group in the surface of the adsorbent [25]. The peaks at  $1992\text{ cm}^{-1}$  and  $2319\text{ cm}^{-1}$  suggested the C-H stretching on the adsorbent surface [27]. A strong intermolecular hydrogen bonding was suggested by the presence of peak at  $3255\text{ cm}^{-1}$  [26, 28]. The presence of these surface active functional groups was mainly responsible for active binding of Cd (II) ion on to the surface of the adsorbent. The functional groups are mostly negatively charged which enhanced the surface binding capacity of the adsorbent for Cd (II). Therefore, the presence of electrostatic interaction was found to be the main mechanism for Cd (II) removal. As described by some previous research work, the presence of surface active functional groups like hydroxyl, carboxylate groups get attached to the protonated surface of

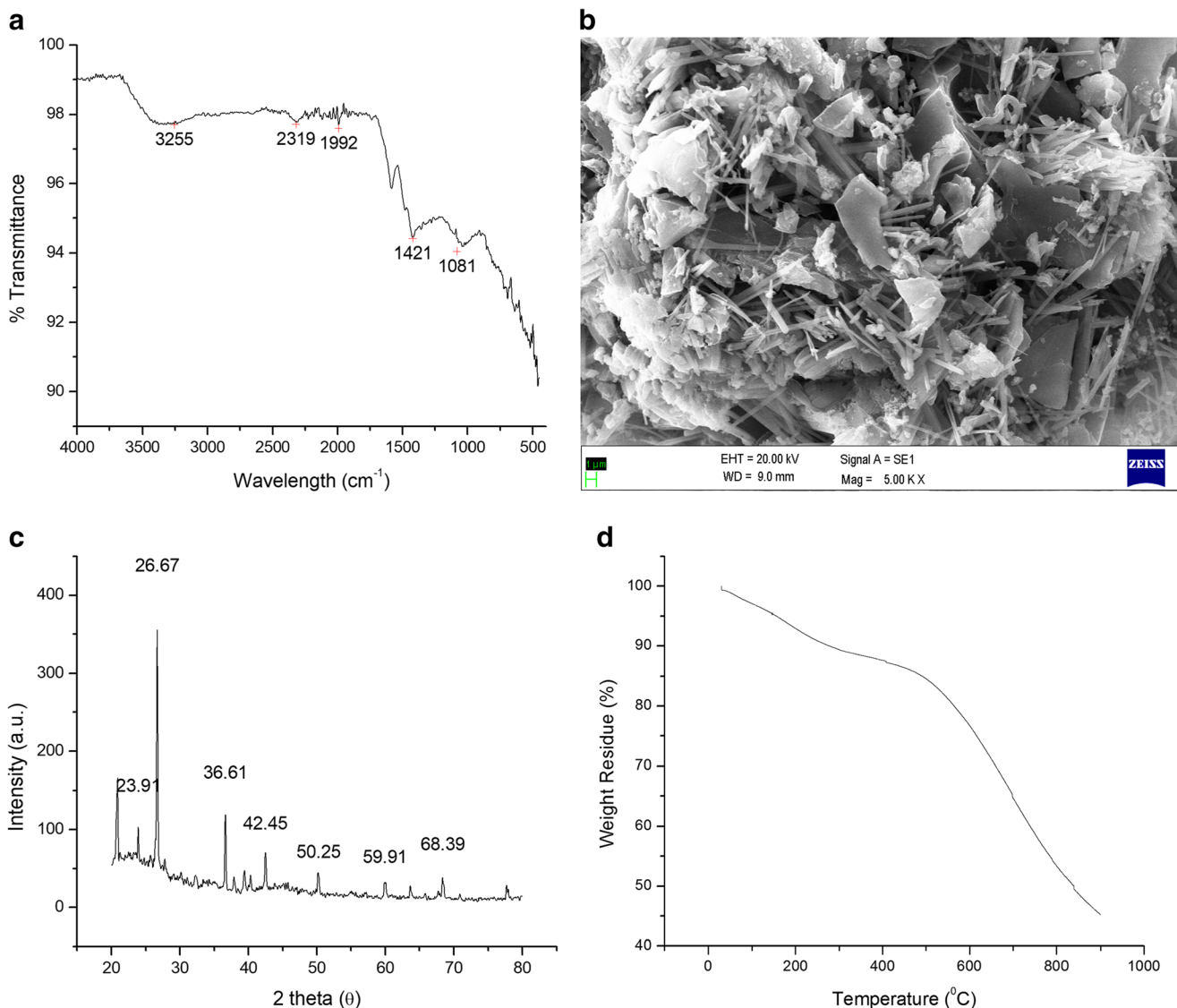


**Fig. 7** a FTIR analysis of SDGO. b SEM image of SDGO. c XRD analysis of SDGO. d TGA analysis of SDGO



**Table 4** Surface structure and pore characteristic of the adsorbent

Sample name	S <sub>BET</sub> (m <sup>2</sup> g <sup>-1</sup> )	Total pore volume (cm <sup>3</sup> g <sup>-1</sup> )
Sawdust graphene oxide composite (SDGO)	97	0.124
Modified sawdust graphene oxide composite (mSDGO)	225.96	0.282

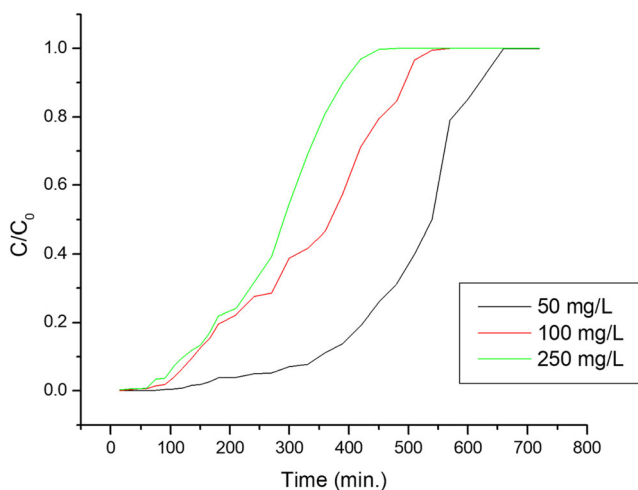
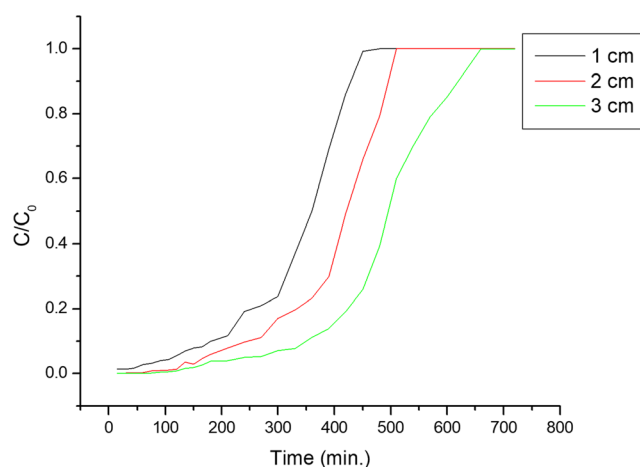
the adsorbate at lower pH, i.e. pH 4, the carboxyl group get deprotonated forming negatively charged COO<sup>-</sup> ion at this lower pH. This negatively charged ion on the surface of the adsorbent may have attracted the positively charged Cd<sup>2+</sup> ion and helped in binding the pollutant in the adsorbent surface.

**SEM analysis** The surface structure and morphology could be suggested by analysing the SEM image (Fig. 7b). It was clear from the image that the surface of the biochar was enhanced by coating it with GO. The porous structure of the biochar was somewhat reduced due to it being coated with GO, but the binding sites were increased due to this surface coating. The presence of graphene sheet on the adsorbent surface was also indicated from the image. The agglomeration of GO on the surface was also seen from the image. The results suggested a good nanocomposite was prepared. The inclusion of graphene oxide into the activated carbon matrix was also suggested previously in some research works [20, 29]. The adsorbent surface was uneven due to carbonization of sawdust. The presence of graphene sheets on the adsorbent surface was clearly seen in the image. The presence of graphene oxide on the adsorbent surface increased the amount of surface functional groups, which increased the adsorption capability of the adsorbent. The presence of pores was also visible from the image which entraps the pollutant into its intricate channels.

**XRD analysis** The crystalline structure of the composite was analysed using XRD analysis (Fig. 7c). The distinct peaks obtained from the result indicated a good crystalline structure

of the composite. The peak at  $2\theta = 26.67^\circ$  suggested a strong presence of crystalline structure of amorphous carbon residue from lignocellulosic waste [13]. The peaks at  $2\theta = 23.91$  and  $42.45$  are the characteristic peaks for GO; this observation was also described by [30]. The peak observed at  $2\theta = 36.61$  indicated the presence of crystalline cellulose [31]. The peaks at  $2\theta = 59.91$  and  $68.38$  indicated the miller indices 511 and 440, which were observed if there was presence of nanoparticles in the carbonaceous sample [13]. The analysis of XRD data could suggest that the carbonization of the biomass was prevalent throughout the adsorbent surface. The formation of amorphous activated carbon had provided the nanocomposite its crystalline structure. The presence of nanoparticles in the adsorbent surface also indicated a good nanocomposite formation, which enhanced the adsorption capability of the adsorbent.

**TGA analysis** The thermal stability of the sample was analysed using TGA (Fig. 7d). The sample was treated in a TGA analyser from 30 to 900 °C. The sample weight loss % was low up to 600 °C; then, a sudden decline in weight was observed which continued till 900 °C. In the initial stage, the weight loss was observed due to evaporation of surface bounded water molecule. The loss of water molecule was observed up to 120 °C [27]. The lignin and hemicellulose were decomposed for a wide range of temperature, starting from 100 to 900 °C. The GO was thermally decomposed at 302 °C. The decomposition was consisted of mainly oxygen-containing functional group [32]. The slow decomposition of

**Fig. 8** Effect of different Cd (II) ion concentrations on breakthrough time at fixed flow rate and bed height**Fig. 9** Effect of different bed heights on breakthrough time for Cd (II) ion solution at fixed flow rate and fixed concentration

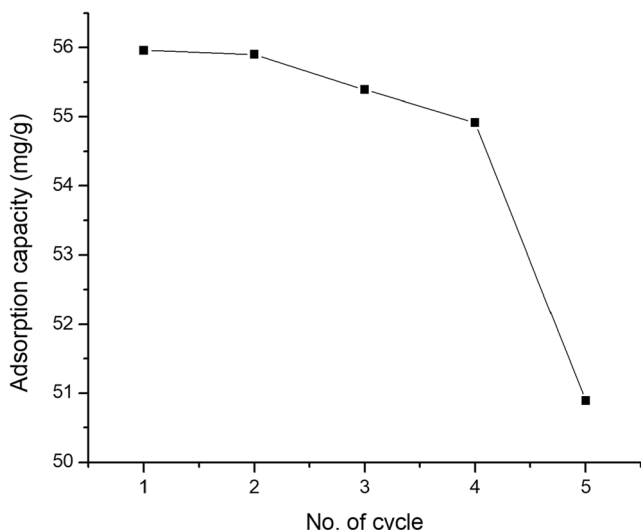


**Fig. 10** Reusability study of the nanocomposite

the adsorbent at this high temperature suggested that the adsorbent had high thermal stability and could be used in a wide range of operation procedures, ranging from lower to higher temperatures. The decomposition mainly took place at temperature above 300 °C. Still there was 50% of the sample left after completing the TGA analysis up to 900 °C.

**BET analysis** The analysis of surface area was found to be one of the most important factors for analysis of surface characteristics. The surface area determines the efficiency of the nanocomposite in removal of pollutants from water. The BET analysis was one of such parameters which determines both the surface area and the pore volume, utilizing nitrogen adsorption method. The results obtained from this study are shown in Table 4. Surface area of this modified SDGO or mSDGO was more as compared to SDGO, i.e. 96.979 m<sup>2</sup>/g for SDGO which increased by 225.96 m<sup>2</sup>/g for mSDGO. The pore volumes of these composites were also increased with the surface area. This increase in surface area helped mSDGO in increasing removal capacity of Cd (II) ion from synthetic water solution.

## 3.2 Fixed-bed column study

### 3.2.1 Effect of concentration in fixed-bed column

Three different concentrations were studied in this column, 50 mg/L, 100 mg/L, and 250 mg/L. The performance of the column was estimated by analysing the breakthrough curve from the graph obtained by plotting the data from column. The effect of metal ion concentration on the column efficiency was studied. In this study except the varying concentrations, all the other parameters were kept constant (pH (7.5), bed height 3 cm was maintained with flow rate 2.5 mL at both inlet and outlet of the column). It was observed that with increase in Cd (II) concentration, there was a fast attaining of breakthrough point for the column. With 50 mg/L of Cd (II) ion concentration, the breakthrough point was observed at 4 h or 240 min, but in the case of 100 mg/L metal ion concentration, the breakthrough point was observed within 100 min, and in the case of 250 mg/L, the breakthrough was obtained within 60 min or 1 h. The breakthrough point was obtained slowly if the concentration was low; that is the ionic interaction was the determining factor for the behaviour of the column. With higher metal ion concentration, there was a first interaction between the nanocomposite and the ions of the metal solution [16]. The competitive adsorption between adsorbent and the adsorbate took place; the binding sites were occupied more quickly with metal ions as compared to the lower metal ion concentrations. The lower the metal ion concentration, the lower the interaction observed between the metal ions and the nanocomposite. In respect of the exhaustion time of the column, the trend was also similar; that is with higher metal ion solution, the exhaustion of column was obtained more quickly than the lower concentrations. The whole study was done for 12 h (720 min). For 50 mg/L the column exhausted in 12 h; in the case of 100 mg/L and 250 mg/L, the column exhaustion time was 570 min and 480 min respectively (Fig. 8). This study provided the efficiency of the column for removing higher metal ion solution (Fig. 8).

**Table 5** Parameters of the (a) Thomas and (b) Adams–Bohart models under different conditions using non-linear regression

C <sub>0</sub> (mg/L)	F (mL/min)	Z (cm)	(a) Thomas model			(b) Adams–Bohart model		
			k <sub>TH</sub> (mL/mg/h)	q <sub>0</sub> max (mg/g)	r <sup>2</sup>	k <sub>AB</sub> (L/mg/h)	N <sub>0</sub> (mg/L)	r <sup>2</sup>
50	2.5	3	0.306	7635.59	0.858	0.000122	832.23	0.8638
100	2.5	3	0.18	32,475.55	0.8564	0.000089	1222.72	0.8011
250	2.5	3	0.0864	64,416.66	0.944	0.00003	3007.61	0.831
50	2.5	2	0.412	8043.53	0.7827	0.000218	1339.94	0.9069
50	2.5	1	0.394	13,729.94	0.7824	0.0002	4665.32	0.9821

C<sub>0</sub> (mg/L), influent strontium concentration; F (mL/min), flow rate (mL/min); H (cm), bed height

### 3.2.2 Effect of bed height in fixed-bed column

The next study for column was done with different bed heights. The study of bed height was also an important parameter for designing a column. For this study, the Cd (II) ion concentration was kept constant, i.e. 50 mg/L, and pH was maintained at 7.5 and flow rate 2.5 mL. The bed heights studied were 1 cm, 2 cm, and 3 cm. The bed height directly relates with the area of exposure for metal ions. The results are shown in Fig. 9. As the bed height increased, the breakthrough time also increased; the breakthrough time was 90 min, whereas for 2 cm bed height was found to be 180 min, which increased up to 360 min for 3-cm bed height. With the increase in bed height, metal ions interacted more with adsorbent surface. The greater the reaction time, the more the efficiency of the column will be [16]. The specific amount of metal ion solution was passed through different bed heights. The numbers of free active sorption sites were more in 3 cm bed height than the other two columns. The reaction time with the nanocomposites was found to be the determining factor for the behaviour of the column. The exhaustion time for the column played another important role for its behaviour. The length of bed height was directly proportional to exhaustion of column. The higher the length of the bed height, the more the exhaustion time. The exhaustion time for 3-cm bed height was 8 h or 720 min, whereas for 2-cm bed height 570 min and for 1-cm bed height the exhaustion time was found to be 480 min (Figs. 9 and 10). So from this study, the relation between the bed height and column behaviour could be estimated.

### 3.2.3 Admas–Bohart model and Thomas model

Both models were studied to know the mechanism of column behaviour. For Admas–Bohart model, the  $k_{AB}$  and  $N_0$  were calculated from the graph plotted using  $C_t/C_0$  vs  $t$ . The value of slope and intercept was used for the calculation of  $k_{AB}$  and  $N_0$ . The values of different concentrations and different bed heights were used in this model. The values of  $k_{AB}$ ,  $N_0$ , and  $R^2$  obtained were plotted in Table 5. It was clear from the values that as the concentration of the metal increases, the  $k_{AB}$  value decreases and  $N_0$  increases. The value of  $R^2$  was high for this model suggesting the model was in good fit for the experiment. The decrease in mass transfer coefficient was inversely proportional with metal ion concentration ([33], Han et al., 2008). The values of  $k_{TH}$  and  $q_0$  were calculated using linear equation, and slope and intercept were used for estimating these parameters; the  $R^2$  value was lower than Admas–Bohart model, indicating that the Thomas model was not appropriate for this study. The data obtained are shown in Table 5.

### 3.3 Regeneration and reusability study of mSDGO

The nanocomposite was able to remove Cd (II) ion from the synthetic waste water for five consecutive cycles. The removal capacity was good in the fifth cycle also. For this reusability study, the adsorbents were simply washed with mild base 0.01 N NaOH and used for the next cycle. The reusability of the adsorbent for pollutant removal was done for making the adsorption process more sustainable and cost effective.

## 4 Conclusion

The biochar obtained from the sawdust was coated with GO using two different processes. The composites which had higher removal capacity for Cd (II) removal were selected for column study. The composites were named SDGO which was synthesized in our previous study [20], and a slight modification in the synthesis procedure was done and a comparison between the two composites was studied. The mSDGO had more removal capacity than SDGO for Cd (II) ion. The surface characteristics were also good as compared with SDGO. When pH range from 6 to 8 was optimized, the removal of Cd (II) ion was done at pH 7.5. The temperature 308.15 K was maintained throughout the experiment. Adsorbent 1 g/L was optimum for the removal of different Cd (II) ion concentrations. The composites can remove up to 500 mg/L of Cd (II) solution efficiently. The equilibrium of this adsorption process was found as 120 min. The adsorption processes followed chemisorption process and were in good fit with Freundlich isotherm process. The process followed pseudo-second-order kinetics and the process was found to be endothermic with increased in randomness in reaction between adsorbent and adsorbate. The column study followed Admas–Bohart model. The column study showed that the composite could be efficiently used in industrial process.

**Funding** The authors are thankful to Science and Engineering Research Board, Department of Science & Technology for financial assistance.

### Compliance with ethical standards

**Conflict of interest** The authors declare that they have no conflict of interest.

## References

- Goel J, Kadirvelu K, Rajagopal C, Garg VK (2006) Cadmium(II) uptake from aqueous solution by adsorption onto carbon aerogel using a response surface methodological approach †. *Ind Eng Chem Res* 45:6531–6537. <https://doi.org/10.1021/ie060010u>
- Inaba T, Kobayashi E, Suwazono Y, Uetani M, Oishi M, Nakagawa H, Nogawa K (2005) Estimation of cumulative cadmium intake

- causing itai–itai disease. *Toxicol Lett* 159:192–201. <https://doi.org/10.1016/j.toxlet.2005.05.011>
3. Jain M, Garg VK, Kadirvelu K (2013) Cadmium(II) sorption and desorption in a fixed bed column using sunflower waste carbon calcium–alginate beads. *Bioresour Technol* 129:242–248. <https://doi.org/10.1016/j.biortech.2012.11.036>
  4. Chowdhury SR, Yanful EK (2013) Kinetics of cadmium(II) uptake by mixed maghemite–magnetite nanoparticles. *J Environ Manag* 129:642–651. <https://doi.org/10.1016/j.jenvman.2013.08.028>
  5. Azouaou N, Sadaoui Z, Djaafri A, Mokaddem H (2010) Adsorption of cadmium from aqueous solution onto untreated coffee grounds: equilibrium, kinetics and thermodynamics. *J Hazard Mater* 184:126–134. <https://doi.org/10.1016/j.jhazmat.2010.08.014>
  6. Bayat M, Beyki MH, Shemirani F (2015) One-step and biogenic synthesis of magnetic Fe<sub>3</sub>O<sub>4</sub>–Fir sawdust composite: application for selective preconcentration and determination of gold ions. *J Ind Eng Chem* 21:912–919. <https://doi.org/10.1016/j.jiec.2014.04.032>
  7. Chakraborty V, Das P, Roy PK (2019) Carbonaceous materials synthesized from thermally treated waste materials and its application for the treatment of strontium metal solution: batch and optimization using response surface methodology. *Environ Technol Innov* 15:100394. <https://doi.org/10.1016/j.eti.2019.100394>
  8. Ekpunobi UE, Agbo SU, Ajiwe VIE (2019) Evaluation of the mixtures of clay, diatomite, and sawdust for production of ceramic pot filters for water treatment interventions using locally sourced materials. *J Environ Chem Eng* 7:102791. <https://doi.org/10.1016/j.jece.2018.11.036>
  9. Yu X, Tong S, Ge M, Zuo J, Cao C, Song W (2013) One-step synthesis of magnetic composites of cellulose@iron oxide nanoparticles for arsenic removal. *J Mater Chem A* 1:959–965. <https://doi.org/10.1039/C2TA00315E>
  10. Taty-Costodes VC, Fauduet H, Porte C, Delacroix A (2003) Removal of Cd(II) and Pb(II) ions, from aqueous solutions, by adsorption onto sawdust of *Pinus sylvestris*. *J Hazard Mater* 105:121–142. <https://doi.org/10.1016/j.jhazmat.2003.07.009>
  11. Wang J, Teng X, Wang H, Ban H (2004) Characterizing the metal adsorption capability of a class F coal fly ash. *Environ Sci Technol* 38:6710–6715. <https://doi.org/10.1021/es049544h>
  12. Hu Z, Qin S, Huang Z, Zhu Y, Xi L, Li Z (2017) Recyclable graphene oxide-covalently encapsulated magnetic composite for highly efficient Pb(II) removal. *J Environ Chem Eng* 5:4630–4638. <https://doi.org/10.1016/j.jece.2017.09.003>
  13. Kataria N, Garg VK (2018) Green synthesis of Fe<sub>3</sub>O<sub>4</sub> nanoparticles loaded sawdust carbon for cadmium (II) removal from water: regeneration and mechanism. *Chemosphere* 208:818–828. <https://doi.org/10.1016/j.chemosphere.2018.06.022>
  14. Wei Yan S, Hoekman K, Broch A, Coronella CJ (2014) Effect of hydrothermal carbonization reaction parameters on the properties of hydrochar and pellets. *Environ Prog Sustain Energy* 33: 676–680. <https://doi.org/10.1002/ep.11974>
  15. Yan W, Hoekman SK, Broch A, Coronella CJ (2014) Effect of hydrothermal carbonization reaction parameters on the properties of hydrochar and pellets. *Environ Prog Sustain Energy* 33:676–680. <https://doi.org/10.1002/ep.11974>
  16. Chowdhury ZZ, Mohd S, Zain S, Rashid AK, Faizur Rafique R, K.K. (2012) Batch and fixed bed adsorption studies of lead (II) cations from aqueous solutions onto granular activated carbon derived from mangostana garcinia shell. *BioResources* 7: 2895–2915.
  17. Bohart GS, Adams EQ (1920) Some aspects of the behavior of charcoal with respect to chlorine. *J Am Chem Soc* 42:523–544. <https://doi.org/10.1021/ja01448a018>
  18. Thomas HC (1944) Heterogeneous ion exchange in a flowing system. *J Am Chem Soc* 66:1664–1666. <https://doi.org/10.1021/ja01238a017>
  19. Devi V, Selvaraj M, Selvam P, Kumar AA, Sankar S, Dinakaran K (2017) Preparation and characterization of CNSR functionalized Fe<sub>3</sub>O<sub>4</sub> magnetic nanoparticles: an efficient adsorbent for the removal of cadmium ion from water. *J Environ Chem Eng* 5: 4539–4546. <https://doi.org/10.1016/j.jece.2017.08.036>
  20. Chakraborty V, Das P, Roy PK (2020) Synthesis and application of graphene oxide coated biochar composite for treatment of strontium-containing solution. *Int J Environ Sci Technol*. <https://doi.org/10.1007/s13762-020-02930-7>
  21. Dada AO, Adekola FA, Odeunmi EO (2017) Liquid phase scavenging of Cd (II) and Cu (II) ions onto novel nanoscale zerovalent manganese (nZVMn): equilibrium, kinetic and thermodynamic studies. *Environ. Nanotechnology. Monit Manag* 8:63–72. <https://doi.org/10.1016/j.enmm.2017.05.001>
  22. Guo S, Jiao P, Dan Z, Duan N, Chen G, Zhang J (2017) Preparation of L-arginine modified magnetic adsorbent by one-step method for removal of Zn(II) and Cd(II) from aqueous solution. *Chem Eng J* 317:999–1011. <https://doi.org/10.1016/j.cej.2017.02.136>
  23. Memon SQ, Memon N, Shah SW, Khuhawar MY, Bhangar MI (2007) Sawdust-a green and economical sorbent for the removal of cadmium (II) ions. *J Hazard Mater* 139:116–121. <https://doi.org/10.1016/j.jhazmat.2006.06.013>
  24. Zheng W, Li XM, Wang F, Yang Q, Deng P, Zeng GM (2008) Adsorption removal of cadmium and copper from aqueous solution by areca-A food waste. *J Hazard Mater* 157:490–495. <https://doi.org/10.1016/j.jhazmat.2008.01.029>
  25. Garg U, Kaur MP, Jawa GK, Sud D, Garg VK (2008) Removal of cadmium (II) from aqueous solutions by adsorption on agricultural waste biomass. *J Hazard Mater* 154:1149–1157. <https://doi.org/10.1016/j.jhazmat.2007.11.040>
  26. Zhang X, Zhang L, Li A (2018) Eucalyptus sawdust derived biochar generated by combining the hydrothermal carbonization and low concentration KOH modification for hexavalent chromium removal. *J Environ Manag* 206:989–998. <https://doi.org/10.1016/j.jenvman.2017.11.079>
  27. Melikoğlu AY, Bilek SE, Cesur S (2019) Optimum alkaline treatment parameters for the extraction of cellulose and production of cellulose nanocrystals from apple pomace. *Carbohydr Polym* 215: 330–337. <https://doi.org/10.1016/j.carbpol.2019.03.103>
  28. Khandanlou R, Ahmad M, Shameli K, Kalantari K (2013) Synthesis and characterization of rice straw/Fe<sub>3</sub>O<sub>4</sub> nanocomposites by a quick precipitation method. *Molecules* 18:6597–6607. <https://doi.org/10.3390/molecules18066597>
  29. Shang M, Liu Y, Liu S, Zeng G, Tan X, Jiang L, Huang X, Ding Y, Guo Y, Wang S (2016) A novel graphene oxide coated biochar composite: synthesis, characterization and application for Cr(VI) removal. *RSC Adv* 88:84562–85674
  30. Deng JH, Zhang XR, Zeng GM, Gong JL, Niu QY, Liang J (2013) Simultaneous removal of Cd(II) and ionic dyes from aqueous solution using magnetic graphene oxide nanocomposite as an adsorbent. *Chem Eng J* 226:189–200. <https://doi.org/10.1016/j.cej.2013.04.045>
  31. Santhi T, Manonmani S, Vasantha VS, Chang YT (2016) A new alternative adsorbent for the removal of cationic dyes from aqueous solution. *Arab J Chem* 9:S466–S474
  32. El Rouby WMA, Farghali AA, Sadek MA, Khalil WF (2018) Fast removal of Sr(II) from water by graphene oxide and chitosan modified graphene oxide. *J Inorg Organomet Polym Mater* 28:2336–2349. <https://doi.org/10.1007/s10904-018-0885-9>
  33. Das P, Das P, Datta S (2016) Continuous biosorption of malachite green by *Ananus comosus* (pineapple) leaf powder in a fixed bed reactor: experimental, breakthrough time and mathematical modeling. *Desalin Water Treat* 57:25842–25847. <https://doi.org/10.1080/19443994.2016.1157040>